

## CHEMICAL BONDING CHARACTER OF THE NETWORK FORMING BONDS IN OXIDE GLASSES

Tokuro Nanba<sup>\*1,\*2</sup>, Shinichi Sakida<sup>\*1</sup>, Yoshinari Miura<sup>\*2</sup>

<sup>\*1</sup> Health and Environment Center, Okayama University  
3-1-1 Tsushima-Naka, Okayama 700-8530, Japan

<sup>\*2</sup> Department of Material and Energy Science, Okayama University  
3-1-1 Tsushima-Naka, Okayama 700-8530, Japan

### ABSTRACT

Chemical bonding character of the glass network forming M–O bonds ( $M = Si, B, Ge$ , and  $Al$ ) was evaluated based on the Mulliken population analyses, in which the bond overlap population  $Q_{MO}$  was obtained from the molecular orbital calculations. It was found in alkali silicates that the interaction of alkali ion with bridging oxygen reduced  $Q_{SiO}$  in  $Si-O-Si$  bridging bonds, and  $Q_{SiO}$  in  $Si-O-Na$  terminal bonds was much larger than that in  $Si-O-Si$  bridges. In  $M-O-M$  bridges, that is,  $Si-O-Si$ ,  $B_3-O-B_3$ ,  $B_4-O-B_4$ ,  $Ge_4-O-Ge_4$  ( $B_n$ ,  $Ge_n$ :  $n$ -fold coordinated boron and germanium),  $Q_{MO}$  was distributed around  $0.6 \pm 0.1$ . In  $M-O-M'$  bridges formed by the heterogeneous combinations of  $B_3-O-B_4$ ,  $Ge_4-O-Ge_5$ ,  $Ge_4-O-Ge_6$ ,  $Si-O-B_4$ , and  $Si-O-Al_4$ ,  $Q_{MO}$  of  $M-O$  bond was larger than  $Q_{M'O}$  of  $M'-O$  bond, and the difference between  $Q_{MO}$  and  $Q_{M'O}$  was about 0.2. It was suggested that the disproportional sharing of electrons reflected the  $\pi$ -bonding character, that is, more electrons were localized on the bonds with larger  $\pi$ -bonding character.

### INTRODUCTION

When alkali oxide such as  $Na_2O$  is added to  $SiO_2$ , bridging oxygens (BOs) in  $Si-O-Si$  bonds are consumed to form non-bridging oxygens (NBOs). NBO possesses a unit negative charge, and alkali ions interact with NBO to compensate the negative charge on NBO. Hence, it has been widely accepted that ionicity of glass increases with increasing alkali content. In  $Na_2O-SiO_2$  glass,<sup>1,2</sup> O1s core-orbital signal observed in XPS is clearly separated into two components assigned to BO and NBO. The relative intensity of the peaks varies depending on the glass composition, and at the same time the peak position also shifts continuously. In general, the peak position, that is, the binding energy of core orbitals is associated with the chemical bonding character and atomic charge.<sup>3,4</sup> For instance, the shift of O1s signal to the lower binding energy side has been routinely interpreted as the increase in electron population of oxide ions which was caused by the increase in ionicity of O–M bonds. It is widely known that O1s signal in  $Na_2O-SiO_2$  glass shifts to lower binding energy side with increasing  $Na_2O$  content. According to the conventional interpretation, the ionicity of the glass increases, that is, oxide ions get more electrons from the neighboring cations, silicon and sodium ions. Hence, the O1s chemical shift experimentally confirmed in  $Na_2O-SiO_2$  glass is apparently consistent with the traditional recognition for the chemical bonding character of glass. If the interpretation is true, the cations should lose electrons and donate them to oxide ions, and it is hence expected that Si2p and Na1s signals shift to the opposite direction from O1s signal. Contrary to the expectation, it

is experimentally confirmed that all the signals shift to the same direction, that is, lower binding energy side with increasing  $\text{Na}_2\text{O}$  content (Figs. 1 and 2).<sup>5</sup>

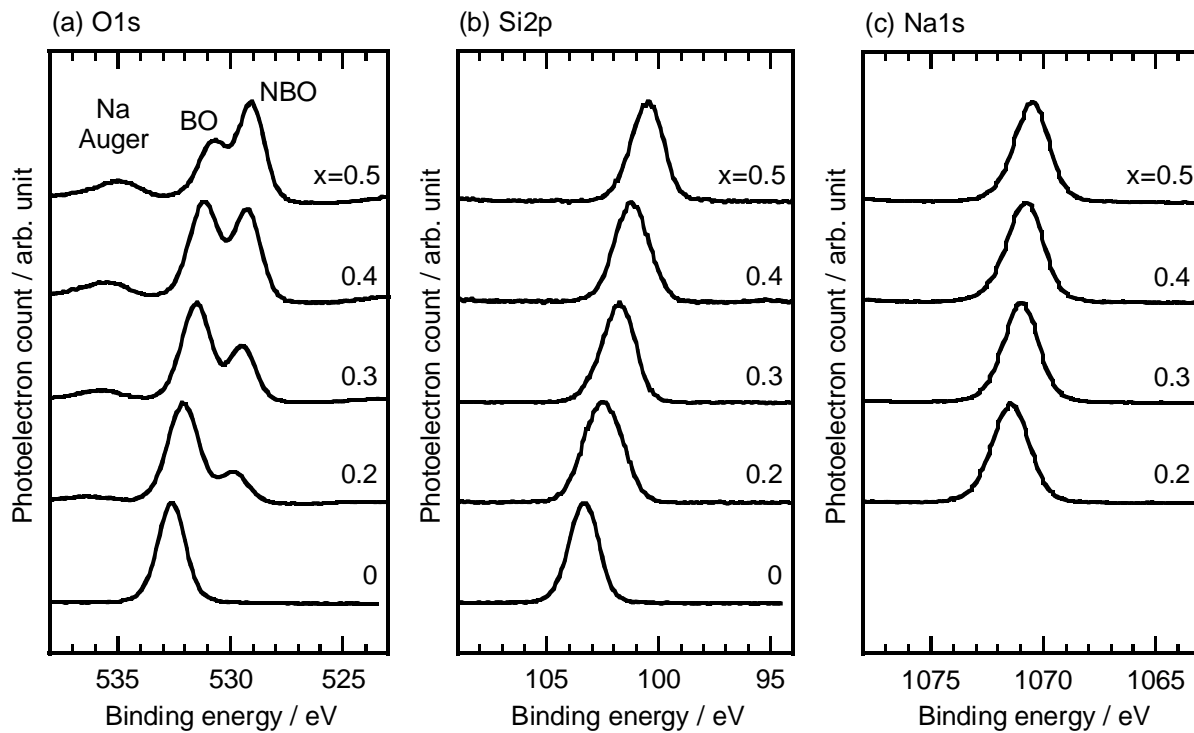


Figure 1. XPS photoelectron spectra for  $x\text{Na}_2\text{O}\cdot(1-x)\text{SiO}_2$  glass.<sup>5</sup>

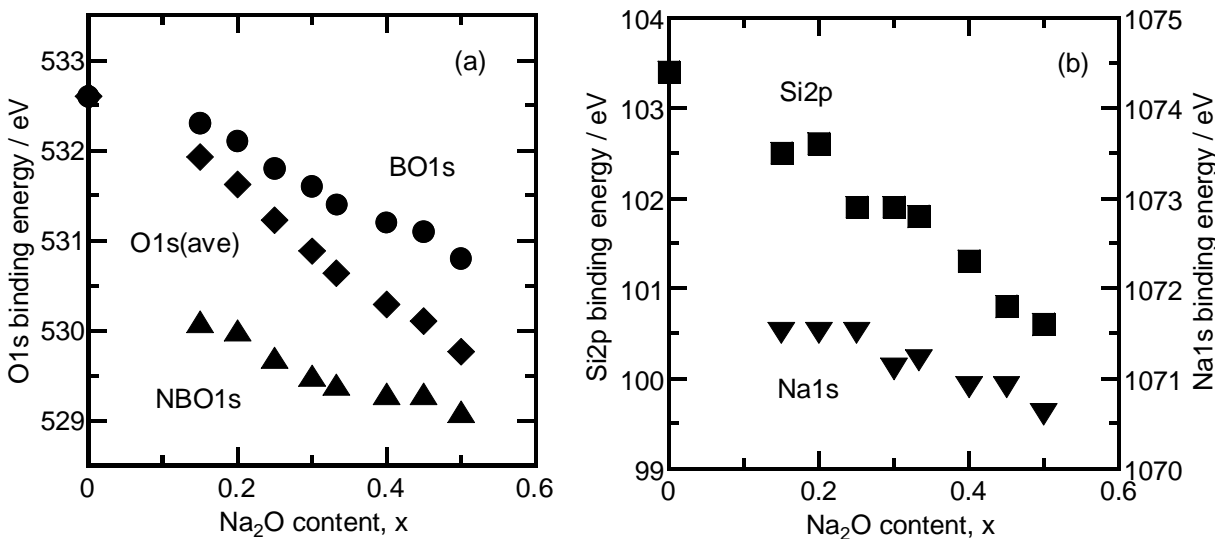


Figure 2. XPS chemical shifts for  $x\text{Na}_2\text{O}\cdot(1-x)\text{SiO}_2$  glass.<sup>5</sup>

For the past decade, the author's research group has been working on the investigation of electronic states and chemical bonding character of various glasses on the basis of experiments and simulations. We have found some inconsistencies between the experimental findings and

conventional understandings.<sup>5,6</sup> The XPS chemical shift above mentioned is an example of the inconsistencies. We have performed molecular orbital (MO) calculations, obtaining theoretical interpretations for the experimental findings.<sup>7-9</sup> In the present paper, the results of the MO calculations are introduced to interpret the chemical bonding characters of the network forming bonds, such as Si–O, B–O, Ge–O, and Al–O bonds in oxide glasses.

## INVESTIGATION PROCEDURES

MO calculations were performed by using the discrete variational X $\alpha$  (DV-X $\alpha$ ) method.<sup>10</sup> It is based on density functional theory, and in the method the Slater's exchange-correlation potential<sup>11</sup>  $V_{xc}(\mathbf{r})$  is used.

$$V_{xc}(\mathbf{r}) = -3\alpha \left\{ \frac{3}{4\pi} \rho(\mathbf{r}) \right\}^{1/3} \quad (1)$$

where  $\rho(\mathbf{r})$  is the electron density at the position  $\mathbf{r}$  and  $\alpha$  is the exchange scaling constant, fixed at 0.7. By virtue of simplicity of the approximate expression, computational time is remarkably reduced, and even in large clusters ab-initio calculations are carried out without any empirical parameters.

Cluster models were constructed from the respective crystal structures. The cluster size, that is, the number of atoms in a cluster was chosen as an objective atom was surrounded by at least two layers of MO<sub>n</sub> network-forming polyhedra. The cluster was also embedded in Madelung potential to reduce the bond termination effects. Chemical bonding character was evaluated by the Mulliken population analysis,<sup>12</sup> and the population analyses were done only for the atoms around the center of the clusters in order to reduce the effects of bond termination. According to the Mulliken population analysis, chemical bonding character of a bond A–B was evaluated by net charge,  $\Delta Q_A$  and bond overlap population,  $Q_{AB}$ ,

$$\Delta Q_A = Z_A - Q_A, \quad Q_A = \sum_{i \in A} Q_i, \quad Q_i = \sum_l Q_i^l, \quad Q_i^l = \sum_j Q_{ij}^l \quad (2)$$

$$Q_{AB} = 2 \sum_{i \in A, j \in B} Q_{ij}, \quad Q_{ij} = \sum_l Q_{ij}^l \quad (3)$$

$$Q_{ij}^l = n_l c_{il} c_{jl} S_{ij} \quad (4)$$

where  $Q_{ij}^l$  is the partial overlap population, that is, electronic population of the overlapped region between the atomic orbitals  $\chi_i$  and  $\chi_j$  in the molecular orbital  $\Phi_l$ , which is the product of  $n_l$ : the number of electrons in MO  $\Phi_l$  (usually  $n_l = 2$ ),  $c_{il}$  and  $c_{jl}$ : the contribution of atomic orbitals  $\chi_i$  and  $\chi_j$  in MO  $\Phi_l$ , and  $S_{ij}$ : the overlap integral between  $\chi_i$  and  $\chi_j$ . In Eq. 2,  $Q_A$  is the gross atomic population or gross atomic charge on an atom A, which is given by the sum of atomic orbital population  $Q_i$ . Subtracting  $Q_A$  from atomic number  $Z_A$ , that is, the number of electrons in the neutral state, the net charge  $\Delta Q_A$  is obtained.

## CHANGE IN THE CHEMICAL BONDING CHARACTER DUE TO ALKALI ADDITION

As mentioned, when an alkali oxide such as Na<sub>2</sub>O is added to SiO<sub>2</sub>, NBOs are formed in SiO<sub>4</sub> units. As shown in Fig. 1, O1s XPS signal is separated into BO and NBO components, and the NBO component increases in relative intensity with increasing Na<sub>2</sub>O content. As also shown

in Fig. 2(a), it is noteworthy that both O1s components shift to a lower binding energy side, suggesting that the electronic state of oxide ions changes continuously along with alkali addition. It is also shown in Fig. 2(b) that Si2p and Na1s signals move in the same direction as O1s signal, indicating an increase in the atomic population, that is, electronic density at outer shells of all the glass constituents, BO, NBO, Si, and Na atoms. This phenomenon is not explainable by the conventional knowledge that the ionicity of chemical bonds in glass increases due to alkali addition. It is therefore assumed that the phenomenon is caused by the increase in bond covalency rather than the increase in bond ionicity; the increase in electrons shared between atoms leads to the increase in atomic population of all the glass constituents.

Then, MO calculations were performed to evaluate the change in the chemical bonding character of Si–O bonds due to the alkali addition,<sup>7</sup> where three cluster models were constructed based on the silicate crystals,  $\alpha$ -cristobalite  $\text{SiO}_2$ ,<sup>13</sup>  $\alpha$ - $\text{Na}_2\text{Si}_2\text{O}_5$ ,<sup>14</sup> and  $\text{Na}_2\text{SiO}_3$ .<sup>15</sup> Overlap population diagrams of Si–O bonds in the clusters are shown in Fig. 3. The BOs in Si–O–Si bridges are classified into two types, that is, BOs associated with no Na atoms (BO1) and BOs associated with Na atoms (BO2). In Fig. 3, bond overlap populations  $Q_{\text{SiO}}$  are also indicated. For example,  $Q_{\text{SiBO1}}$  in  $\text{SiO}_2$  is 0.628, which is obtained by the sum of  $Q_{\text{SiO}}$  of bonding (positive) and anti-bonding (negative) overlaps, 0.654 – 0.025.  $Q_{\text{SiO}}$  increases in the order of Si–BO2, Si–BO1 and Si–NBO, indicating that the terminal Si–NBO bonds have higher covalency than the bridging Si–BO bonds. The contribution of anti-bonding overlap on overlap population diagram is small but clearly seen around the top of the occupied levels ( $\sim 5$  eV) in Si–BO bonds. With increasing  $\text{Na}_2\text{O}$  content,  $Q_{\text{SiBO1}}$  decreases and  $Q_{\text{SiNBO}}$  increases, but the variations are quite small. The variation in  $Q_{\text{SiBO2}}$  along is larger as compared with the other Si–O bonds. As shown in Fig. 4, BO2 in  $\text{Na}_2\text{Si}_2\text{O}_5$  is associated with one Na atom, but BO2 in  $\text{Na}_2\text{SiO}_3$  has two Na atoms as neighbors. It is suggested that the interaction with alkali ions enhances anti-bonding overlap in Si–BO bonds and weakens Si–O–Si bridges, and it is also expected that Si–O–Si bridges are broken to form terminal Si–NBO bonds when BO meets three or more Na atoms.

According to the variation in the bond overlap population  $Q_{\text{SiO}}$  along with alkali addition, Si–NBO bonds increases slightly in  $Q_{\text{SiO}}$ , indicating an increase in bond covalency, and Si–BO bonds, however, decreases in  $Q_{\text{SiO}}$ , indicating a decrease in bond covalency. As shown in Fig. 2, both the O1s components BO and NBO move to the same direction, which tells us the XPS chemical shift is not simply interpreted by the chemical bonding character. The XPS chemical shift is also discussed based on atomic charge.<sup>4</sup> According to the MO calculations, the net charge  $\Delta Q_A$  estimated from Eq. 2 decreases for Si, Na and BO with increasing  $\text{Na}_2\text{O}$  content, but only NBO shows the opposite change in  $\Delta Q_A$ . The decrease in  $\Delta Q_A$  means acquisition of electrons which are donated from or shared with the neighbors. The decrease of  $\Delta Q_A$  for Si results from the increase in the total amount of electrons shared with the neighboring oxygen atoms. The gross atomic population given by Eq. 2 is rewritten as  $Q_A = Q_{AA} + \frac{1}{2}\sum Q_{AB}$ , where  $Q_{AA}$  is the net atomic population, that is, the electronic population localized on atom A and is also given by Eq. 3. Si atoms in  $\text{SiO}_4$  units have no lone pair electrons so that the variation in  $Q_{AA}$  is negligible and the total amount of shared electrons  $\frac{1}{2}\sum Q_{AB}$  dominates  $Q_A$ . When NBO is formed in an  $\text{SiO}_4$  unit, that is, Si–NBO bond replaces Si–BO bond,  $\frac{1}{2}\sum Q_{\text{SiO}}$  for Si in the  $\text{SiO}_4$  unit increases, since  $Q_{\text{SiNBO}}$  is much higher than  $Q_{\text{SiBO}}$ . Finally, the net charge of Si,  $\Delta Q_{\text{Si}}$

decreases along with the formation of NBO, resulting in the lower binding energy shift of Si2p XPS signal in glass.

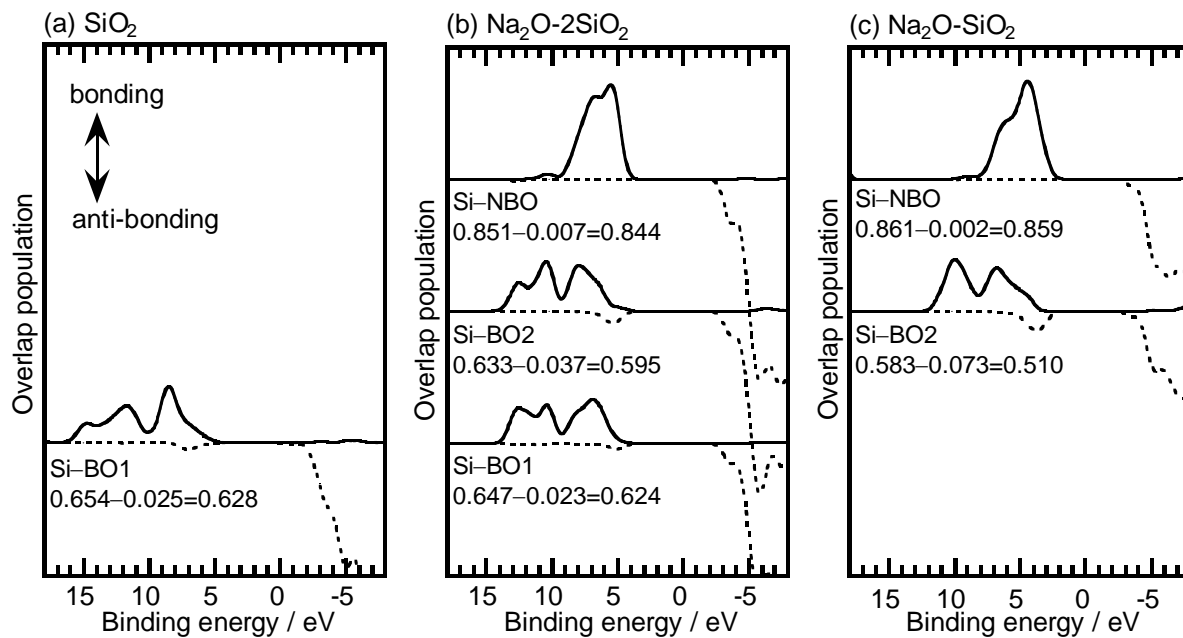


Figure 3. Overlap population diagrams of Si–O bonds in the cluster models constructed from the silicate crystals, (a)  $\alpha$ -cristobalite  $\text{SiO}_2$ , (b)  $\alpha$ - $\text{Na}_2\text{Si}_2\text{O}_5$ , and (c)  $\text{Na}_2\text{SiO}_3$ . BO1 and BO2 represent the bridging oxygen atoms associated without and with Na atoms, respectively. The continuous and broken lines indicate bonding and anti-binding overlap, respectively. The numerical values indicate the bond overlap population,  $Q_{\text{SiO}}$  estimated from Eq. 3.

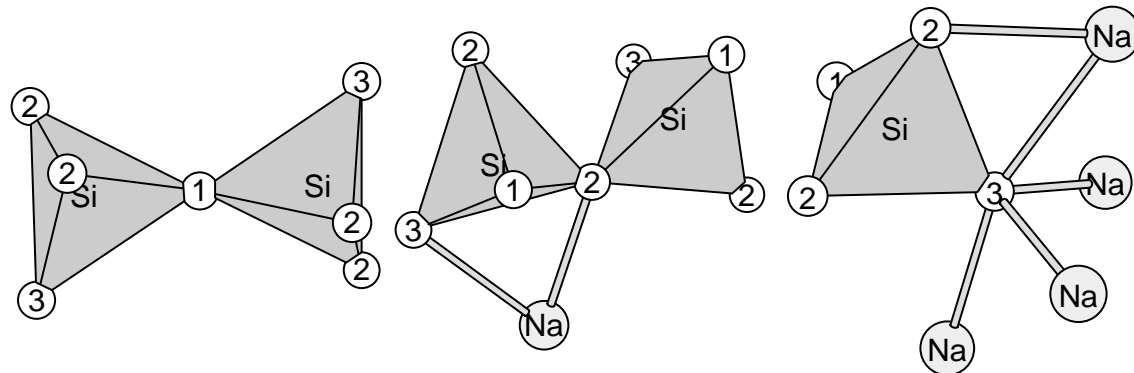


Figure 4. Three oxygen sites in  $\alpha$ - $\text{Na}_2\text{Si}_2\text{O}_5$ . 1: bridging oxygen (BO1 in Fig. 3), 2: bridging oxygen associated with Na (BO2 in Fig. 3), 3: non-bridging oxygen (NBO in Fig. 3).

## CHEMICAL BONDING CHARACTER AND COORDINATION STRUCTURE

It is well known that the coordination number of boron atoms changes along with alkali addition; in alkali-free glass, boron atoms take the coordination number of 3, and the relative amount of tetrahedral boron atoms,  $N_4$  ( $= [\text{B}4]/[\text{B}3]+[\text{B}4]$ ), increases without forming NBOs until alkali content = 30 mol% ( $B_n$ :  $n$ -fold coordinated boron). Only at higher alkali content,  $N_4$  decreases with the formation of NBOs. In alkali germanate glasses, the structural changes along

with the composition are quite similar to borate glasses; it has been commonly accepted that Ge atoms take the coordination numbers of 4 and 6 in glass, but recently it was reported that 5-fold coordinated Ge atoms were produced ahead of octahedral Ge atoms.<sup>16</sup> In general, properties of glass change monotonically depending on the composition, and in the case of borate and germanate glasses, however, extrema are often observed in various properties, such as thermal expansion coefficient and electrical conductivity. Those phenomena are well-known as borate and germanate anomalies. The anomalies were initially associated with the structural changes, but it was revealed that neither the change in coordination number nor the formation of NBO were the direct cause.<sup>17</sup> In alkali borate glasses, the coordination number of boron reaches a maximum at 30 ~ 40 mol% of alkali oxide addition, and the extrema in properties are frequently observed at much less addition around 15 ~ 20 mol%. The anomalies in borate and germanate glasses should be interpreted based on the chemical bonding character and electronic states rather than the coordination structures. It is still undoubted that the electronic structure of a material depends on the atomic structure.

Then, the chemical bonding character was evaluated for the various bonding groups in borate and germanate crystals. Among borate crystals, pure  $B_2O_3$  and diborate compositions were chosen. As for the pure  $B_2O_3$ , the crystals so-called " $B_2O_3$ -I" and " $B_2O_3$ -II" were investigated.  $B_2O_3$ -I<sup>18</sup> is constructed by  $BO_3$  triangles, but the boroxol rings which are confirmed in glass are not present in this crystal.  $B_2O_3$ -II<sup>19</sup> is a high pressure form, in which only tetrahedral  $BO_4$  units form the network sharing their corners. In  $B_2O_3$ -II, there are two oxygen sites; one is coordinated by two  $B_4$  atoms forming  $B_4-O-B_4$  bridges, and the other is coordinated by three  $B_4$  atoms forming  $B_4-O(-B_4) \times 2$ , so-called "tricluster" units (Fig. 5). The tricluster oxygen has not been confirmed experimentally in borate glasses. It was assumed in borosilicate glasses,<sup>20</sup> but it should not be abundant even if present. Among the diborate crystals, Li, Na and K diborates were examined. Besides the boroxol group, various borate groups are found in borate glasses; for instance, diborate group in  $Li_2OB_4O_7$ ,<sup>21</sup> dipentaborate group and triborate group with NBO in  $Na_2OB_4O_7$ ,<sup>22</sup> and ditriborate group in  $K_2OB_4O_7$ .<sup>23</sup> These borate groups are formed by  $B_3-O-B_3$ ,  $B_3-O-B_4$ , and  $B_4-O-B_4$  bridges. Chemical bonding character of these bonds was evaluated by the MO calculations.

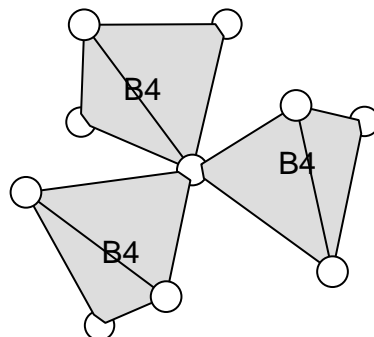


Figure 5.  $BO_4$  "Tricluster" unit present in  $B_2O_3$ - II.<sup>19</sup>

The bond overlap population  $Q_{B3O}$  of  $B_3-O$  bonds in  $B_3-O-B_3$  bridges is 0.64 in  $B_2O_3$ -I and 0.59 in  $Na_2B_4O_7$  ( Fig. 6). As shown in Fig. 3,  $Q_{SiO}$  of  $Si-O$  bonds in  $Si-O-Si$  bridges decreases along with the  $Na_2O$  addition, which is due to the interaction with Na ions. In  $Na_2B_4O_7$  crystal, oxygen atoms in  $B_3-O-B_3$  bridges have an average of 1.5 Na ions as

neighbors, and it is therefore concluded that the decrease in  $Q_{B3O}$  in B3–O–B3 bridges is also caused by the interaction with alkali ions. Unfortunately, B3–O–B3 bridges are absent in  $\text{Li}_2\text{B}_4\text{O}_7$  and  $\text{K}_2\text{B}_4\text{O}_7$  crystals so that the dependence of alkali species on  $Q_{B3O}$  is not discussed. B4–O–B4 bridges are, however, commonly present in the diborate crystals, in which the difference in  $Q_{B4O}$  is smaller than 0.5 and Li-diborate shows higher  $Q_{B4O}$  than the other Na- and K-diborates. Except for B4–O–B4 in  $\text{B}_2\text{O}_3$ -II,  $Q_{B4O}$  in B4–O–B4 bridges is smaller than  $Q_{B3O}$  in B3–O–B3 bridges. In general,  $Q_{AB}$  decreases with lengthening a bond A–B. The average B–O bond length is 0.139 nm in B3–O–B3 bridges and 0.145 nm in B4–O–B4 bridges. The general trend in  $Q_{AB}$  is also applicable to B–O bonds.

As compared with  $Q_{B3O}$  in B3–O–B3 bridge and  $Q_{B4O}$  in B4–O–B4 bridge, the difference between  $Q_{B3O}$  and  $Q_{B4O}$  in B3–O–B4 bridge is quite large;  $0.68 - 0.48 = 0.20$  in Li-diborate,  $0.67 - 0.50 = 0.17$  in Na-diborate, and  $0.67 - 0.49 = 0.18$  in K-diborate. It means unequal electron sharing between B3–O and B4–O bonds in a B3–O–B4 bridge. In addition,  $Q_{B3O}$  in B3–O–B4 which is shown by B3–O(–B4) in Fig. 6 is higher than that in B3–O–B3, and  $Q_{B4O}$  in B3–O–B4 is smaller than that in B4–O–B4. As mentioned, B4–O bonds are longer than B3–O bonds, but the difference in bond length between B3–O and B4–O is significantly developed in B3–O–B4 bridge. It is supposed that the disproportion of  $Q_{BO}$  in B3–O–B4 bridge results from the difference in bonding character between B3–O and B4–O; in the conventional notation, B3 is in  $\text{sp}^2$  hybrid, and hence the vacant B3 2p<sub>z</sub> overlaps with the neighboring O2p lone pairs, forming  $\pi$ -bonds. B4 is in  $\text{sp}^3$  hybrid, and the  $\pi$ -bonding character of B4–O is therefore much smaller than that of B3–O. Consequently, electrons are disproportionately distributed between B3–O and B4–O bonds in B3–O–B4 bridge.

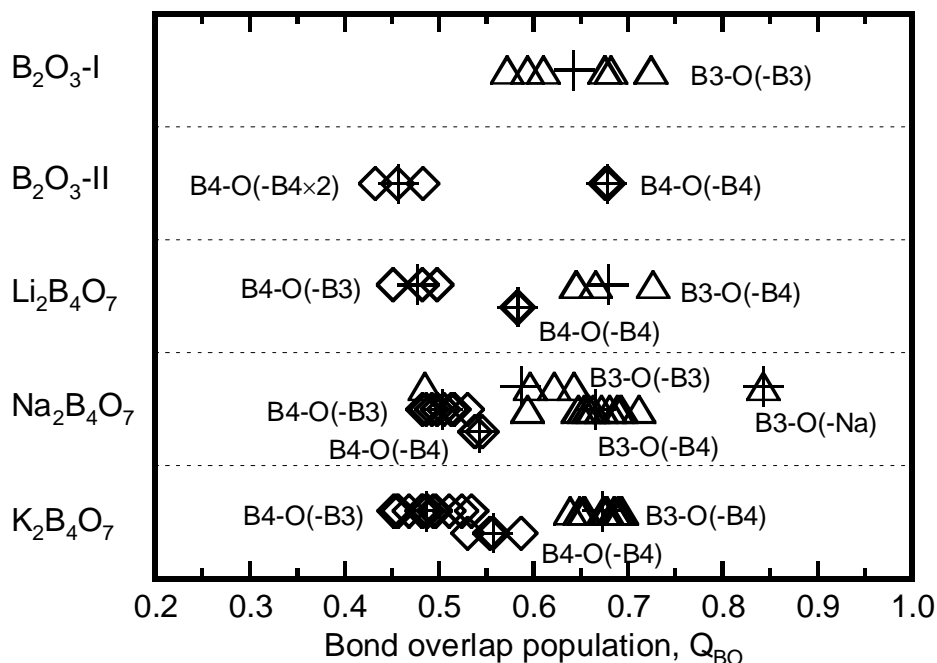


Figure 6. Bond overlap population of boron–oxygen bonds,  $Q_{BO}$ , obtained from the MO calculations.  $Bn$  represents  $n$ -fold coordinated boron, and  $Bn$ –O(– $Bm$ ) indicates  $Bn$ –O bond in  $Bn$ –O– $Bm$  bridge. Cross markers indicate the average of open markers.

It is expected that there exists a similarity in the bonding character between the borate and germanate systems, because the compositional dependence of coordination number is in a similar fashion. If the bonding character is different, it is probably due to the difference in  $\pi$ -bonding character. In borates, B<sub>3</sub>–O bonds in trigonal BO<sub>3</sub> units have higher  $\pi$ -bonding character than B<sub>4</sub>–O bonds in tetrahedral BO<sub>4</sub> units, which is due to the overlap between vacant B<sub>2</sub>p<sub>z</sub> and O<sub>2</sub>p perpendicular to the BO<sub>3</sub> triangle. In germanates, high  $\pi$ -bonding character in Ge<sub>4</sub>–O bonds in GeO<sub>4</sub> units is not expected, but Ge<sub>6</sub>–O bonds in GeO<sub>6</sub> units may have a higher  $\pi$ -bonding character than Ge<sub>4</sub>–O bonds, because Ge has a vacant 4d orbital which is available to form  $\pi$ -bonds. On the other hand, octahedral Ge<sub>6</sub> atoms are sometimes regarded as a network modifier; if such the perspective is appropriate, Ge<sub>6</sub>–O bonds should have much smaller bond overlap population than Ge<sub>4</sub>–O bonds.

MO calculations were performed for the cluster models constructed from the germanate crystals with various coordination structures. Quartz-GeO<sub>2</sub><sup>24</sup> consists of tetrahedral GeO<sub>4</sub> units sharing their corners. Rutile-GeO<sub>2</sub><sup>25</sup> is formed by octahedral GeO<sub>6</sub> units sharing their edges, where oxygen atoms are coordinated by three Ge<sub>6</sub> atoms. Among the alkali germanate binary crystals, K<sub>2</sub>Ge<sub>8</sub>O<sub>17</sub><sup>26</sup> is the only crystal containing 5-fold coordinated Ge<sub>5</sub> atoms, in which two GeO<sub>5</sub> units share an edge between the units forming a dimeric [Ge<sub>2</sub>O<sub>8</sub>]<sup>8-</sup> unit (Fig. 7b). Oxygen atoms shown by Ge<sub>5</sub>–O(–Ge<sub>5</sub>) in Fig. 8 are located on the edge. Na<sub>4</sub>Ge<sub>9</sub>O<sub>20</sub><sup>27</sup> is formed by GeO<sub>4</sub> and GeO<sub>6</sub> units, where four GeO<sub>6</sub> units gather together forming a large tetragonal tetramer [Ge<sub>4</sub>O<sub>16</sub>]<sup>16-</sup> unit (Fig. 7c).

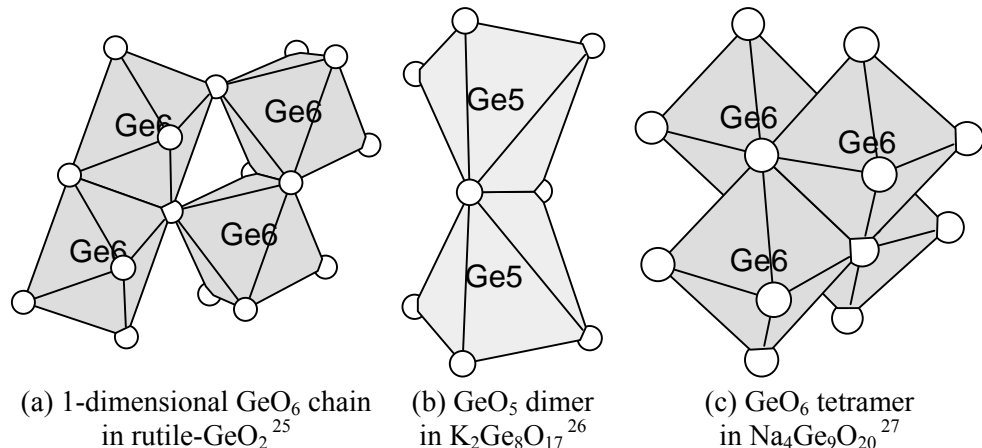


Figure 7. Various edge sharing units present in the germanate crystals.

The bond overlap population of Ge–O bonds,  $Q_{\text{GeO}}$  is summarized in Fig. 8. Except for rutile-GeO<sub>2</sub>, Ge<sub>4</sub>–O–Ge bridges are commonly present in the crystals investigated, and the difference in  $Q_{\text{Ge}4\text{O}}$  between the crystals is quite small, indicating the small influence of alkali ions on the bonding character of Ge<sub>4</sub>–O bonds.  $Q_{\text{Ge}6\text{O}}$  in Ge<sub>6</sub>–O(–Ge<sub>6</sub>×2) is different between rutile-GeO<sub>2</sub> and Na<sub>4</sub>Ge<sub>9</sub>O<sub>20</sub> crystals, which is probably due to the difference in coordination structures rather than the interaction of alkali ions; in rutile-GeO<sub>2</sub>, GeO<sub>6</sub> units form 1-dimensional chains sharing their edges (Fig. 7a). As for the oxygen atoms coordinated by the Ge atoms with different coordination numbers, such as Ge<sub>4</sub>–O–Ge<sub>5</sub> and Ge<sub>4</sub>–O–Ge<sub>6</sub>, a similar trend is observed, which is previously seen in B<sub>3</sub>–O–B<sub>4</sub> bridges. In Ge<sub>4</sub>–O–Ge<sub>5</sub> bridge,  $Q_{\text{Ge}4\text{O}}$

is larger than  $Q_{\text{Ge}5\text{O}}$ , and is also larger than  $Q_{\text{Ge}4\text{O}}$  in Ge4–O–Ge4 bridge. A similar result is observed in Ge4–O–Ge6 bridge, but the difference in  $Q_{\text{GeO}}$  between Ge4–O–Ge4 and Ge4–O–Ge6 bridges in Na<sub>4</sub>Ge<sub>9</sub>O<sub>20</sub> is quite small as compared with K<sub>2</sub>Ge<sub>8</sub>O<sub>17</sub>. Higher  $\pi$ -bonding character of Ge6–O bonds may be a reason for the difference in chemical bonding character between Ge6–O–Ge4 and Ge5–O–Ge4 bridges, and the actual reason is, however, still unexplained.

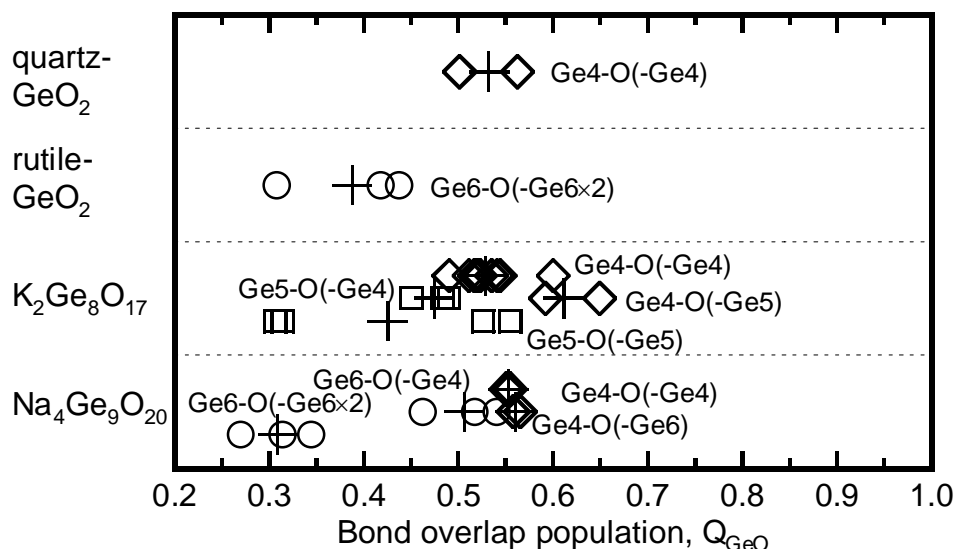
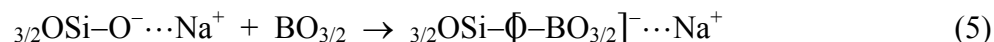


Figure 8. Bond overlap population of germanium–oxygen bonds,  $Q_{\text{BO}}$ , obtained from the MO calculations. Gen represents  $n$ -fold coordinated germanium, and Gen–O(–Gem) indicates Gen–O bond in Gen–O–Gem bridge. Cross markers indicate the average of open markers.

#### MIXED NETWORK FORMER EFFECT ON THE CHEMICAL BONDING CHARACTER

It is widely known that NBO reduces chemical durability and mechanical strength of glass. As compared with BO, more electrons are localized on NBO as non-bonding lone pair electrons in O2p orbitals, which are located at around the HOMO levels. With increasing NBO concentration, the gap between the HOMO-LUMO levels decreases and the reactivity of a material increases. For the purpose of improving the chemical durability and mechanical strength, B<sub>2</sub>O<sub>3</sub> or Al<sub>2</sub>O<sub>3</sub> is often added to a glass, reducing the NBO concentration.



where Si–O terminal bonds are replaced by Si–O–B4 or Si–O–Al4 bridging bonds. Eq. 5 is based on the assumption that boron and aluminum atoms added occupy tetrahedral site, and the tetrahedral B4 and Al4 atoms are exclusively coordinated by BOs.

Subject to Eq. 5, NBO concentration decreases with increasing B<sub>2</sub>O<sub>3</sub> and Al<sub>2</sub>O<sub>3</sub> contents, and it is expected that NBO disappears at B<sub>2</sub>O<sub>3</sub>/Na<sub>2</sub>O or Al<sub>2</sub>O<sub>3</sub>/Na<sub>2</sub>O = 1. In practice, the NBO elimination was confirmed at Al<sub>2</sub>O<sub>3</sub>/Na<sub>2</sub>O = 1 in aluminosilicate glasses,<sup>28</sup> and in borosilicate glasses, however, NBO remained at B<sub>2</sub>O<sub>3</sub>/Na<sub>2</sub>O = 1.<sup>29</sup> It is known that Al atom takes the coordination numbers of 4, 5, and 6 in glass, and tetrahedral Al atoms have been conventionally

regarded as a network former. At  $\text{Al}_2\text{O}_3/\text{Na}_2\text{O} \leq 1$  in aluminosilicate glasses, all Al atoms take 4-fold coordination. As described, boron takes 3- and 4-fold coordination, and to the authors' knowledge,  $N_4$  (fraction of B4) in glass has never attained to 1.0, indicating that boron atoms in glass preferentially occupy the trigonal sites. The difference in preferential coordination structures between B and Al is probably caused by the difference in chemical bonding character. Then, the chemical bonding characters of B–O and Al–O bonds in borosilicate and aluminosilicate materials were investigated by MO calculation.

According to Yun and Bray,<sup>30</sup> a structural group,  $\text{B}(\text{SiO}_4)_4$  are commonly present in borosilicate glasses. In  $\text{B}(\text{SiO}_4)_4$  unit, a  $\text{BO}_4$  unit is surrounded by four  $\text{SiO}_4$  units, and the unit is present in a borosilicate mineral, reedmergnerite  $\text{NaBSi}_3\text{O}_8$ . Then, cluster models were constructed based on the crystal,  $\text{NaBSi}_3\text{O}_8$ .<sup>31</sup> According to Aoki et al.,<sup>32</sup>  $\text{Na}_2\text{O}\cdot\text{Al}_2\text{O}_3\cdot 2\text{SiO}_2$  glass has a very similar structure to an aluminosilicate mineral, nepheline  $\text{KNa}_3\text{Al}_4\text{Si}_4\text{O}_{16}$  among the several aluminosilicate minerals. Cluster models were therefore constructed based on the nepheline structure.<sup>33</sup> In the crystal,  $\text{SiO}_4$  and  $\text{AlO}_4$  units are alternately arranged, and Si–O–Al4 bridging bonds are exclusively present.

Fig. 9 shows the bond overlap population,  $Q_{\text{MO}}$ . As for Si–O bonds, when the second neighboring atom, M of Si, ( $\text{Si}-\text{O}-\text{M}$ ) is different ( $\text{M} = \text{B}4$  and  $\text{Al}4$ ), the Si–O bonds show different  $Q_{\text{SiO}}$ ;  $Q_{\text{SiO}}$  in  $\text{Si}-\text{O}-\text{B}4$  is larger than that in  $\text{Si}-\text{O}-\text{Al}4$ . In  $\text{Si}-\text{O}-\text{B}4$  bridge, the Si–O and B4–O bonds show different  $Q_{\text{MO}}$ , and it is also the case in  $\text{Si}-\text{O}-\text{Al}4$  bridge. Such the disproportion in  $Q_{\text{MO}}$  was also found in  $\text{B}3-\text{O}-\text{B}4$  (Fig. 6),  $\text{Ge}4-\text{O}-\text{Ge}5$ , and  $\text{Ge}4-\text{O}-\text{Ge}6$  bridges (Fig. 8). It was tentatively concluded that the difference in  $\pi$ -bonding character was responsible for the electronic disproportion. The disproportion in  $\text{Si}-\text{O}-\text{B}4$  bridge is explainable by the difference in  $\pi$ -bonding characters between Si–O and B4–O bonds. Tetrahedral boron has no vacant atomic orbitals, such as  $\text{B}2\text{p}_z$  in trigonal boron, which are available for  $\pi$ -bonds. According to Uchino et al.,<sup>34</sup> electrons are delocalized through  $\text{Al}3\text{d}$  orbitals in aluminosilicates. If  $\text{Al}4-\text{O}$  bonds had higher  $\pi$ -bonding character than  $\text{B}4-\text{O}$  bonds, the difference between  $Q_{\text{Al}4\text{O}}$  and  $Q_{\text{SiO}}$  in  $\text{Al}4-\text{O}-\text{Si}$  bridge would be smaller than the that between  $Q_{\text{B}4\text{O}}$  and  $Q_{\text{SiO}}$  in  $\text{B}4-\text{O}-\text{Si}$  bridge. As shown in Fig. 9, however, the differences of  $Q_{\text{MO}}$  in these bridges are not so different (~0.2).

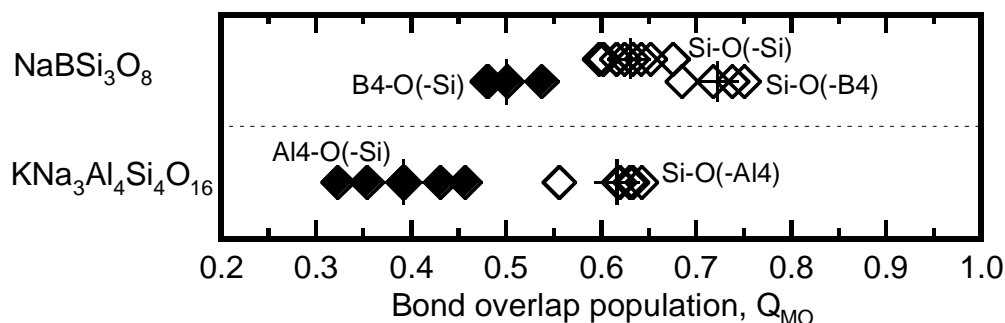


Figure 9. Bond overlap population of M–O bonds,  $Q_{\text{MO}}$ , ( $\text{M} = \text{Al}4$ ,  $\text{B}4$ , and Si) obtained from the MO calculations. Cross markers indicate the average of open markers.

According to Lippmaa et al.,<sup>35 29</sup>  $^{29}\text{Si}$  NMR chemical shift in aluminosilicates ranges over  $-86 \sim -110$  ppm, and it depends on the number of Al atoms at the second neighboring sites. The chemical shift for Si atoms which have 3 or 4 Al atoms as second neighbors overlaps with that of

Si atoms associated with one NBO (so-called Q<sup>3</sup> Si) ( $-85 \sim -92$  ppm in alkali silicate glasses<sup>36</sup>). It is interpreted that more electrons are localized on the Si–O bonds in Si–O–Al<sub>4</sub> bridge than the Si–O bonds in Si–O–Si bridge, and hence <sup>29</sup>Si NMR peak moves to the higher relative frequency side with increasing the number of Al atoms at the second neighboring sites. It is likely to happen in borosilicates, because, as shown in Fig. 9, more electrons are localized on the Si–O bonds in Si–O–B<sub>4</sub> bridge than the Si–O bonds in Si–O–Si bridge. In <sup>29</sup>Si NMR analyses of borosilicate glasses, the peak assignments should be done with enough care.

## CONCLUSION

Chemical bonding character of the glass network forming M–O bonds (M = Si, B, Ge, and Al) was evaluated based on the bond overlap population  $Q_{MO}$  estimated from the molecular orbital calculations. In alkali silicates,  $Q_{SiO}$  in Si–O–Si bridging bonds decreased and Si–O–Si bridges gradually weakened with increasing alkali content, which resulted from the increase in anti-bonding overlap due to the interaction between bridging oxygen and alkali ions. In Si–O–Na terminal bonds, however,  $Q_{SiO}$  increased with increasing alkali content. It was finally concluded that the bonding character of Si–O networks as a whole increased in covalency and strengthened, which was opposite to the conventional understanding.

The disproportionate sharing of electrons was commonly observed in the bridging bonds formed by the heterogeneous combinations, B<sub>3</sub>–O–B<sub>4</sub>, Ge<sub>4</sub>–O–Ge<sub>5</sub>, Ge<sub>4</sub>–O–Ge<sub>6</sub>, Si–O–B<sub>4</sub>, and Si–O–Al<sub>4</sub>, and  $Q_{MO}$  in the bridging bonds of the homogeneous combinations, Si–O–Si, B<sub>3</sub>–O–B<sub>3</sub>, B<sub>4</sub>–O–B<sub>4</sub>, Ge<sub>4</sub>–O–Ge<sub>4</sub>, was observed at the intermediate positions between  $Q_{MO}$  and  $Q_{M' O}$  in M–O–M' bridge. It was tentatively concluded that the disproportion was caused by the difference in bonding character, and many electrons were localized on the bonds with larger  $\pi$ -bonding character. In M–O–M bridges,  $Q_{MO}$  ranged at  $0.6 \pm 0.1$ , and the distribution seemed to be narrow as compared with the covalency expected from electronegativities. This might be another glass forming condition, that is, only the M–O bonds with  $Q_{MO} \sim 0.6$  participated in glass networks.

## ACNOWLEDGMENT

The authors would like to thank Mr. Tatsuya Hagiwara, Ms. Akiko Mano, and Mr. Masahiro Nakamura for the collaboration in molecular orbital calculations.

## REFERENCES

- <sup>1</sup>R. Brückner, H.U. Chun, and H. Goretzki, *Glastechn. Ber.*, **49**, 211-3 (1976).
- <sup>2</sup>R. Brückner, H.U. Chun, and H. Goretzki, *Glastechn. Ber.*, **51**, 1-7 (1978).
- <sup>3</sup>K. Siegbahn, C. Nordling, G. Johansson, J. Hedman, P.F. Hedén, K. Hamrin, U. Gelius, T. Bergmark, L.O. Werme, R. Manne, and Y. Baer, *ESCA applied to free molecules*; pp.104-9, North-Holland Publ. Co., New York, 1969.
- <sup>4</sup>U. Gelius, P.F. Hedén, J. Hedman, B.J. Lindberg, R. Manne, R. Nordberg, C. Nordling, and K. Siegbahn, “Molecular Spectroscopy by Means of ESCA. III. Carbon compounds,” *Physica Scripta*, **2**, 70-80 (1970).
- <sup>5</sup>S. Matsumoto, T. Nanba, and Y. Miura, “X-Ray Photoelectron Spectroscopy of Alkali Silicate Glasses,” *J. Ceram. Soc. Japan*, **106**, 415-21 (1998) (in Japanese), *J. Ceram. Soc. Jpn. Int. Ed.*, **106**, 439-45 (1998) (in English).

- <sup>6</sup>T. Nanba and Y. Miura, "Alkali Distribution in Borosilicate Glasses," *Phys. Chem. Glasses*, **44**, 244-8 (2003).
- <sup>7</sup>T. Nanba, T. Hagiwara, and Y. Miura, "Chemical bonding state of sodium silicates," *Adv. Quantum Chem.*, **42**, 187-98 (2003).
- <sup>8</sup>T. Nanba, M. Nishimura, and Y. Miura, "A theoretical interpretation of the chemical shift of <sup>29</sup>Si NMR peaks in alkali borosilicate glasses," *Geochim. Cosmochim. Acta*, **68**, 5103-11 (2004).
- <sup>9</sup>T. Nanba and Y. Miura, "Chemical bonding character of aluminosilicate glasses"; in *Proc. XX Intern. Congr. Glass*, O-10-038, Kyoto, Japan, 2004 (CD-ROM).
- <sup>10</sup>H. Adachi, M. Tsukada, and C. Satoko, "Discrete Variational X $\alpha$  Cluster Calculations. I. Application to Metal Clusters," *J. Phys. Soc. Japan*, **45**, 875-83 (1978).
- <sup>11</sup>J.C. Slater, *The Self-Consistent Field For Molecules and Solids*, McGraw-Hill, New York, 1974.
- <sup>12</sup>R.S. Mulliken, "Electronic Population Analysis on LCAO-MO Molecular Wave Functions," *J. Chem. Phys.*, **23**, 1833-40, 1841-6, 2338-42, and 2343-6 (1955).
- <sup>13</sup>R.W.G. Wyckoff, *Crystal Structures*, vol.1, p.316, Interscience Publishers, New York, 1965.
- <sup>14</sup>A.K. Pant and D.W.J. Cruickshank, "The crystal structure of  $\alpha$ -Na<sub>2</sub>Si<sub>2</sub>O<sub>5</sub>," *Acta Cryst.*, **B24**, 13-9 (1968).
- <sup>15</sup>P.A. Grund and M.M. Pizy, "Structure cristalline du metasilicate de sodium anhydre, Na<sub>2</sub>SiO<sub>3</sub>," *Acta Cryst.*, **5**, 837-40 (1952).
- <sup>16</sup>H.M. Wang and G.S. Henderson, "Investigation of coordination number in silicate and germanate glasses using O K-edge X-ray absorption spectroscopy," *Chem. Geol.*, **213**, 17-30 (2004).
- <sup>17</sup>S.A. Feller, W.J. Dell, and P.J. Bray, "<sup>10</sup>B NMR studies of lithium borate glasses," *J. Non-Cryst. Solids*, **51**, 21-30 (1982).
- <sup>18</sup>G.E. Gurr, P.W. Montgomery, C.D. Knutson, and B.T. Gorres, "The crystal structure of trigonal diboron trioxide," *Acta. Cryst.*, **B26**, 906-15 (1970).
- <sup>19</sup>C.T. Prewitt and R.D. Shannon, "Crystal structure of a high-pressure form of B<sub>2</sub>O<sub>3</sub>," *Acta. Cryst.*, **B24**, 869-74 (1968).
- <sup>20</sup>P. Zhao, S. Kroeker, and J.F. Stebbins, "Non-bridging oxygen sites in barium borosilicate glasses: Results from <sup>11</sup>B and <sup>17</sup>O NMR," *J. Non-Cryst. Solids*, **276**, 122-31 (2000).
- <sup>21</sup>J. Krogh-Moe, "Refinement of the crystal structure of lithium diborate Li<sub>2</sub>O·2B<sub>2</sub>O<sub>3</sub>," *Acta. Cryst.*, **B24**, 179-81 (1968).
- <sup>22</sup>J. Krogh-Moe, "The crystal structure of sodium diborate, Na<sub>2</sub>O·2B<sub>2</sub>O<sub>3</sub>," *Acta. Cryst.*, **B30**, 578-82 (1974).
- <sup>23</sup>J. Krogh-Moe, "The crystal structure of potassium diborate, K<sub>2</sub>O·2B<sub>2</sub>O<sub>3</sub>," *Acta. Cryst.*, **B28**, 3089-93 (1972).
- <sup>24</sup>G.S. Smith and P.B. Isaacs, "The crystal structure of quartz-like GeO<sub>2</sub>," *Acta Cryst.*, **17**, 842-46 (1964).
- <sup>25</sup>W.H. Baur and A.A. Khan, "Rutile-type compounds. IV. SiO<sub>2</sub>, GeO<sub>2</sub> and a comparison with other rutile-type structures," *Acta Cryst.*, **B27**, 2133-9 (1971).
- <sup>26</sup>V.E. Fáy, H. Völlenkle, and A. Wittmann, "Die Kristallstruktur des Kaliumoktagermanats, K<sub>2</sub>Ge<sub>8</sub>O<sub>17</sub>," *Zeit. Krist.*, **138**, 439-48 (1973).
- <sup>27</sup>N. Ingri and G. Lundgren, "The Crystal Structure of Na<sub>4</sub>Ge<sub>9</sub>O<sub>20</sub>," *Acta Chem. Scand.*, **17**, 617-33 (1963).

- <sup>28</sup>Y. Miura, S. Matsumoto, T. Nanba, and T. Akazawa, "X-ray photoelectron spectroscopy of sodium aluminosilicate glasses," *Phys. Chem. Glasses*, **41**, 24-31 (2000).
- <sup>29</sup>Y. Miura, H. Kusano, T. Nanba, and S. Matsumoto, "X-ray photoelectron spectroscopy of sodium borosilicate glasses," *J. Non-Cryst. Solids*, **290**, 1-14 (2001).
- <sup>30</sup>Y.H. Yun and B.J. Bray, "Nuclear magnetic resonance studies of the glasses in the system Na<sub>2</sub>O-B<sub>2</sub>O<sub>3</sub>-SiO<sub>2</sub>," *J. Non-Cryst. Solids*, **27**, 363-80 (1978).
- <sup>31</sup>D.E. Appleman, and J.R. Clark, "Crystal structure of reedmergnerite, a boron albite, and its relation to feldspar crystal chemistry," *Am. Mineral.*, **50**, 1827-50 (1965).
- <sup>32</sup>N. Aoki, S. Yambe, H. Inoue, H. Hasegawa, and I. Yasui, "An X-ray diffraction study of the structure of Na<sub>2</sub>O, Al<sub>2</sub>O<sub>3</sub>, 2SiO<sub>2</sub> glass," *Phys. Chem. Glasses*, **27**, 124-7 (1986).
- <sup>33</sup>T. Hahn and M.J. Buerger, "The Detailed Structure of Nepheline, KNa<sub>3</sub>Al<sub>4</sub>Si<sub>4</sub>O<sub>16</sub>," *Z. Kristallogr.*, **106**, 308-38 (1955).
- <sup>34</sup>T. Uchino, T. Sakka, Y. Ogata, and M. Iwasaki, "Local structure of sodium aluminosilicate glass: an ab initio molecular orbital study," *J. Phys. Chem.*, **97**, 9642-9 (1993).
- <sup>35</sup>E. Lippmaa, M. Maegi, A. Samoson, M. Tarmak, and G. Engelhardt, "Investigation of the structure of zeolites by solid-state high-resolution silicon-29 NMR spectroscopy," *J. Am. Chem. Soc.*, **103**, 4992-6 (1981).
- <sup>36</sup>H. Maekawa, T. Maekawa, K. Kawamura, and T. Yokokawa, "The structural groups of alkali silicate glasses determined from <sup>29</sup>Si MAS-NMR," *J. Non-Cryst. Solids*, **127**, 53-64 (1991).